

Vector Signal Reconstruction Sparse and Parametric Approach of direction of arrival Using Single Vector Hydrophone

Jiabin Guo¹

¹ *Acoustic Science and Technology Laboratory, Harbin Engineering University, Harbin, 150001, China*

This article discusses the application of single vector hydrophones in the field of underwater acoustic signal processing for Direction Of Arrival (DOA) estimation. Addressing the limitations of traditional DOA estimation methods in multi-source environments and under noise interference, this study introduces a Vector Signal Reconstruction Sparse and Parametric Approach (VSRSPA). This method involves reconstructing the signal model of a single vector hydrophone, converting its covariance matrix into a Toeplitz structure suitable for the Sparse and Parametric Approach (SPA) algorithm. The process then optimizes it using the SPA algorithm to achieve more accurate DOA estimation.

Through detailed simulation analysis, this research has confirmed the performance of the proposed algorithm in single and dual-target DOA estimation scenarios, especially under various signal-to-noise ratio(SNR) conditions. The simulation results show that, compared to traditional DOA estimation methods, this algorithm has significant advantages in estimation accuracy and resolution, particularly in multi-source signals and low SNR environments. The contribution of this study lies in providing an effective new method for DOA estimation with single vector hydrophones in complex environments, introducing new research directions and solutions in the field of vector hydrophone signal processing.

I. INTRODUCTION

In the field of underwater acoustic signal processing, Direction of Arrival (DOA) estimation is an important part of array signal processing. It serves as the premise and foundation for underwater acoustic target identification, localization, and tracking, aiming to acquire the target's bearing information from signals received by spatially distributed array elements. Compared to scalar hydrophones that can only measure sound pressure information in the sound field, vector hydrophones are capable of simultaneously measuring both sound pressure and particle velocity at the same point. Single vector hydrophones possess frequency-independent dipole directivity and certain capabilities to resist isotropic noise. These characteristics enable single vector hydrophones to achieve unambiguous direction finding across the entire space, effectively addressing the issue of limited array aperture in underwater acoustic detection on small platforms. Therefore, the research and application of single vector hydrophones, especially in underwater acoustic DOA, have attracted widespread attention in recent years¹⁻⁴.

Common DOA estimation methods, such as the Multiple Signal Classification (MUSIC)⁵ algorithm and the Estimation of Signal Parameters via Rotational Invariance Techniques (ESPRIT)⁶ algorithm, have been proven to possess high resolution and accuracy in multi-source environments. Such algorithms provide a theoretical foundation for the application of single vector hydrophones in DOA estimation. G.L. D'Spain conducted a comparative analysis of beamforming results between single vector hydrophones and vector hydrophone arrays⁷. Wang *et al.* explored the application of the Minimum Variance Distortionless Response (MVDR) beamforming technique to single gradient vector hydrophone signal processing⁸. Tichavsky *et al.* proposed an ESPRIT algorithm based on single vector hydrophones⁹, while Levin introduced a single vector hydrophone DOA estimation method based on maximum likelihood estimation¹⁰. Liang *et al.* applied the MUSIC algorithm to single vector hydrophones and proposed an improved algorithm¹¹. Addressing the issue of

inconsistent noise power between the sound pressure channel and the particle velocity channel in single vector hydrophones, Liu *et al.* proposed a MUSIC algorithm that eliminates false sources¹². Chen *et al.* applied matrix filters to single vector hydrophones, enhancing the performance of the MUSIC algorithm¹³.

Although traditional methods rely on single vector hydrophones to measure components of sound pressure and particle velocity to estimate the position of sound sources, these methods often face many challenges in complex environments, especially in multi-source environments and under noise interference. Due to the unique array orientation vector structure of single vector hydrophones, and the fact that, even without channel amplitude errors, the noise power received by the sound pressure and particle velocity channels in isotropic noise environments remains different, the existing algorithms widely used for array Direction of Arrival (DOA) estimation are difficult to apply directly to single vector hydrophones¹⁰⁻¹².

The development of sparse signal processing techniques has provided new solutions for DOA (Direction of Arrival) estimation methods. In recent years, algorithms related to sparse signal processing have been widely applied to array-based DOA estimation¹⁴⁻¹⁸, utilizing the sparsity of spatial signals to improve the performance of target bearing estimation. These algorithms can effectively enhance the accuracy and resolution of estimations under the premise of unknown signal sparse distribution¹⁹⁻²¹. Recently, researchers have begun to explore the possibility of applying these algorithms to single vector hydrophones. Wang *et al.* has utilized a single vector hydrophone, employing the Sparse Asymptotic Minimum Variance (SAMV) algorithm for target bearing estimation²². In recent years, gridless sparse methods, such as the Sparse and Parametric Approach (SPA)¹⁶, have shown significant potential in the field of array signal processing. The application of these methods is currently mainly limited to Uniform Linear Arrays (ULA) and Sparse Linear Arrays (SLA). This limitation is mainly because these methods depend on specific mathematical structures,

such as the Vandermonde decomposition of the Toeplitz covariance matrix, which is easily satisfied in the case of ULA and SLA²³⁻²⁷. However, the signal processing model of single vector hydrophones does not directly conform to this structure, preventing gridless sparse methods from being directly applied to DOA estimation problems for single vector hydrophones.

In order to facilitate the application of such algorithms on single vector hydrophones and inspired by the processing of combined channels of sound pressure and particle velocity in vector hydrophones^{28,29}, this paper proposes a novel vector signal reconstruction method, distinct from the aforementioned approaches. Our method introduces complex operations and proposes a technique for vector signal reconstruction, restructuring the signal of a single vector hydrophone. It converts the covariance matrix of the single vector received signal into a Toeplitz structure suitable for such methods. Further, we introduce the Vector Signal Reconstruction Sparse and Parametric Approach (VSRSPA), which, compared to traditional algorithms, effectively enhances estimation accuracy and resolution probability in environments with multiple sources and low signal-to-noise ratio(SNR).

The purpose of this article is to provide a detailed introduction to the theoretical foundations and implementation details of the vector signal reconstruction method, and to verify its effectiveness in practical applications through simulation results. Through comparative analysis, we will demonstrate the significant advantages of the VSRSPA algorithm over traditional DOA estimation methods in terms of direction estimation accuracy and resolution, especially highlighting its application potential in multi-source and low SNR environments.

II. SINGLE VECTOR HYDROPHONE SIGNAL MODEL

Consider a two-dimensional vector hydrophone composed of a sound pressure sensor and two vector velocity sensors that are perpendicular to each other on the horizontal plane. The output of the vector hydrophone contains three information channels: the sound pressure channel (p -

channel), the x -axis velocity channel (x -channel), and the y -axis velocity channel (y -channel).

Assuming that there are K mutually independent far-field signals $s_k(t), k = 1, 2, \dots, K$ within the spatial domain of the vector hydrophone, then the received signal model of the two-dimensional single vector hydrophone (which measures the sound pressure and the horizontal components of particle velocity) can be represented as:

$$\begin{aligned} \mathbf{x}(t) &= \begin{bmatrix} p(t) \\ v_x(t) \\ v_y(t) \end{bmatrix} \\ &= \sum_{k=1}^K \mathbf{a}(\theta_k) s_k(t) + \mathbf{n}(t) \\ &= \mathbf{A}(\boldsymbol{\theta}) \mathbf{s}(t) + \mathbf{n}(t) \end{aligned} \tag{1}$$

Here, $\mathbf{x}(t)$ represents the signal received by the hydrophone at time t . The direction vector $\mathbf{a}(\theta_k) = [1, \cos \theta_k, \sin \theta_k]^T$ is a 3×1 dimensional vector, and $\mathbf{A}(\boldsymbol{\theta}) = [\mathbf{a}(\theta_1), \dots, \mathbf{a}(\theta_K)]$. $\mathbf{s}(t) = [s_1(t), \dots, s_K(t)]^T$ denotes the received signal vector, and $\mathbf{n}(t)$ is a 3×1 dimensional noise vector, assumed to be zero-mean additive Gaussian white noise. The signals and noise are considered to be uncorrelated.

Assuming that DOA estimation is performed with T snapshots, then the received signal model can be represented as:

$$\mathbf{X} = \mathbf{A}(\boldsymbol{\theta}) \mathbf{S} + \mathbf{N} \tag{2}$$

$\mathbf{X} = [\mathbf{x}(1), \mathbf{x}(2), \dots, \mathbf{x}(T)]$, $\mathbf{S} = [\mathbf{s}(1), \mathbf{s}(2), \dots, \mathbf{s}(T)]$ and $\mathbf{N} = [\mathbf{n}(1), \mathbf{n}(2), \dots, \mathbf{n}(T)]$,

the covariance matrix of $\mathbf{x}(t)$ can be represented as:

$$\begin{aligned}
\mathbf{R}_x &= E[\mathbf{x}(t)\mathbf{x}^H(t)] \\
&= \sum_{k=1}^K \sigma_{sk}^2 \mathbf{a}(\theta_k)\mathbf{a}(\theta_k)^H + E[\mathbf{n}(t)\mathbf{n}(t)^H] \\
&= \mathbf{A}(\vartheta) \begin{bmatrix} \sigma_{s1}^2 & 0 & \cdots & 0 \\ 0 & \sigma_{s2}^2 & \cdots & \vdots \\ \vdots & \vdots & \ddots & 0 \\ 0 & \cdots & 0 & \sigma_{sK}^2 \end{bmatrix} \mathbf{A}^H(\vartheta) + \begin{bmatrix} \sigma_{np}^2 & 0 & 0 \\ 0 & \sigma_{nx}^2 & 0 \\ 0 & 0 & \sigma_{ny}^2 \end{bmatrix} \\
&= \sum_{k=1}^K \sigma_{sk}^2 \begin{bmatrix} 1 & \cos\theta_k & \sin\theta_k \\ \cos\theta_k & \cos^2\theta_k & \cos\theta_k\sin\theta_k \\ \sin\theta_k & \sin\theta_k\cos\theta_k & \sin^2\theta_k \end{bmatrix} + \begin{bmatrix} 1 & 0 & 0 \\ 0 & 1/2 & 0 \\ 0 & 0 & 1/2 \end{bmatrix} \sigma_n^2 \\
&= \mathbf{R}_s + \mathbf{R}_n
\end{aligned} \tag{3}$$

Where $\sigma_{sk}^2, k = 1, 2, \dots, K$, represents the signal power of the k th source. $\sigma_{np}^2, \sigma_{nx}^2, \sigma_{ny}^2$ respectively represent the noise power of the sound pressure channel, the velocity x channel, and the velocity y channel. The signal covariance matrix \mathbf{R}_s and the noise covariance matrix \mathbf{R}_n can be represented as follows:

$$\begin{aligned}
\mathbf{R}_s &= \sum_{k=1}^K \sigma_{sk}^2 \begin{bmatrix} 1 & \cos\theta_k & \sin\theta_k \\ \cos\theta_k & \cos^2\theta_k & \cos\theta_k\sin\theta_k \\ \sin\theta_k & \sin\theta_k\cos\theta_k & \sin^2\theta_k \end{bmatrix} \\
\mathbf{R}_n &= \begin{bmatrix} 1 & 0 & 0 \\ 0 & 1/2 & 0 \\ 0 & 0 & 1/2 \end{bmatrix} \sigma_n^2
\end{aligned} \tag{4}$$

III. SPARSE AND PARAMETRIC ESTIMATION ALGORITHM BASED ON VECTOR SIGNAL RECONSTRUCTION

The key advantage of the SPA algorithm lies in its ability to avoid parameter discretization, thereby reducing computational burden and modeling error. To adapt the SPA algorithm, vector signal reconstruction technology optimizes the traditional single vector signal model by transforming the covariance matrix into the required Toeplitz structure, solving the issue that the standard model does not meet this structural requirement.

A. Vector Signal Reconstruction Method

Upon re-examining the structure of the signal covariance matrix \mathbf{R}_s , it does not fully satisfy all the requirements of a Toeplitz structure. Specifically, the definition of \mathbf{R}_s is as follows:

$$\mathbf{R}_s = \sum_{k=1}^K \sigma_{s_k}^2 \begin{bmatrix} 1 & \cos \theta_k & \sin \theta_k \\ \cos \theta_k & \cos^2 \theta_k & \cos \theta_k \sin \theta_k \\ \sin \theta_k & \sin \theta_k \cos \theta_k & \sin^2 \theta_k \end{bmatrix} \quad (5)$$

For a Toeplitz structure, its key characteristic is that the elements on each diagonal of the matrix should be the same. In \mathbf{R}_s , the off-diagonal elements are equal to the elements in symmetric positions to the diagonal, partially satisfying the characteristics of a Toeplitz structure. However, the diagonal elements of \mathbf{R}_s are not uniform, for example, the main diagonal elements are 1 , $\cos^2 \theta_k$, and $\sin^2 \theta_k$. The Toeplitz structure requires uniformity in the matrix's diagonal elements, which is not fully realized in \mathbf{R}_s . Thus, although \mathbf{R}_s approximates a Toeplitz structure to some extent, it does not completely conform to the standard definition of a Toeplitz matrix.

One of the key characteristics of a Toeplitz structure is that the elements on each diagonal of the matrix should be the same. In \mathbf{R}_s , despite the off-diagonal elements being equal to their symmetrical counterparts across the diagonal, showing certain symmetry, the diagonal elements of \mathbf{R}_s are not uniform, such as the different presentations of 1 , $\cos^2 \theta_k$, and $\sin^2 \theta_k$. Another characteristic of the Toeplitz structure is the requirement for uniformity in the diagonal elements, which is not exhibited in \mathbf{R}_s . Therefore, although \mathbf{R}_s demonstrates certain symmetrical characteristics, it does not fully meet the definition of a Toeplitz matrix.

Considering the requirements of the SPA algorithm, this paper proposes a method for vector signal reconstruction. This method utilizes a specific vector signal reconstruction matrix \mathbf{G} , which transforms the single vector received data $\mathbf{x}(t)$ by left multiplication, aiming to reconstruct the

covariance matrix of the single vector received signal into a Toeplitz structure suitable for the SPA algorithm. The vector signal reconstruction matrix \mathbf{G} is defined as follows:

$$\mathbf{G} = \begin{bmatrix} 0 & 1 & -j \\ 1 & 0 & 0 \\ 0 & 1 & j \end{bmatrix} \quad (6)$$

The construction of this matrix is achieved by combining the velocity x channel and the velocity y channel signal components of the single vector hydrophone to create a new complex signal representation. In practical applications, the matrix \mathbf{G} performs a left multiplication operation on the single vector received data $\mathbf{x}(t)$, thereby generating a new signal vector $\mathbf{y}(t) = \mathbf{G}\mathbf{x}(t)$. This transformation not only retains the key information of the original data but also provides a suitable mathematical framework for further signal analysis and processing.

$$\begin{aligned} \mathbf{y}(t) &= \mathbf{G}\mathbf{x}(t) \\ &= \mathbf{G} \begin{bmatrix} p(t) \\ v_x(t) \\ v_y(t) \end{bmatrix} \\ &= \mathbf{G} \left(\sum_{k=1}^K \begin{bmatrix} 1 \\ \cos(\theta_k) \\ \sin(\theta_k) \end{bmatrix} s_k(t) + \mathbf{n}(t) \right) \\ &= \begin{bmatrix} 0 & 1 & -j \\ 1 & 0 & 0 \\ 0 & 1 & j \end{bmatrix} \left(\sum_{k=1}^K \begin{bmatrix} 1 \\ \cos(\theta_k) \\ \sin(\theta_k) \end{bmatrix} s_k(t) + \mathbf{n}(t) \right) \\ &= \begin{bmatrix} \sum_{k=1}^K \cos(\theta_k) s_k(t) - j \sum_{k=1}^K \sin(\theta_k) s_k(t) \\ \sum_{k=1}^K s_k(t) \\ \sum_{k=1}^K \cos(\theta_k) s_k(t) + j \sum_{k=1}^K \sin(\theta_k) s_k(t) \end{bmatrix} + \begin{bmatrix} 0 & 1 & -j \\ 1 & 0 & 0 \\ 0 & 1 & j \end{bmatrix} \mathbf{n}(t) \end{aligned} \quad (7)$$

By utilizing Euler's formula $e^{j\theta} = \cos(\theta) + j\sin(\theta)$ and $e^{-j\theta} = \cos(\theta) - j\sin(\theta)$, the formula can be further simplified to yield the following expression:

$$\mathbf{y}(t) = \sum_{k=1}^K \begin{bmatrix} e^{-j\theta_k} s_k(t) \\ s_k(t) \\ e^{j\theta_k} s_k(t) \end{bmatrix} + \mathbf{G}\mathbf{n}(t) \quad (8)$$

Through vector signal reconstruction, the covariance matrix of the single vector data received can be represented as:

$$\begin{aligned} \mathbf{R}_y &= \mathbb{E}[\mathbf{y}(t)\mathbf{y}^H(t)] \\ &= \mathbb{E}[\mathbf{G}\mathbf{x}(t)(\mathbf{G}\mathbf{x}(t))^H] \\ &= \mathbb{E}[\mathbf{G}\mathbf{x}(t)\mathbf{x}^H(t)\mathbf{G}^H] \\ &= \mathbf{G}\mathbf{R}_x\mathbf{G}^H \\ &= \mathbf{G}(\mathbf{R}_s + \mathbf{R}_n)\mathbf{G}^H \\ &= \mathbf{G}\mathbf{R}_s\mathbf{G}^H + \mathbf{G}\mathbf{R}_n\mathbf{G}^H \\ &= \mathbf{G} \left(\sum_{k=1}^K \sigma_{s_k}^2 \begin{bmatrix} 1 & \cos\theta_k & \sin\theta_k \\ \cos\theta_k & \cos^2\theta_k & \cos\theta_k \sin\theta_k \\ \sin\theta_k & \sin\theta_k \cos\theta_k & \sin^2\theta_k \end{bmatrix} \right) \mathbf{G}^H + \mathbf{G} \left(\begin{bmatrix} 1 & 0 & 0 \\ 0 & 1/2 & 0 \\ 0 & 0 & 1/2 \end{bmatrix} \sigma_n^2 \right) \mathbf{G}^H \\ &= \sum_{k=1}^K \sigma_{s_k}^2 \begin{bmatrix} 1 & e^{-j\theta} & e^{-j2\theta} \\ e^{j\theta} & 1 & e^{-j\theta} \\ e^{j2\theta} & e^{j\theta} & 1 \end{bmatrix} + \sigma_n^2 \begin{bmatrix} 1 & 0 & 0 \\ 0 & 1 & 0 \\ 0 & 0 & 1 \end{bmatrix} \end{aligned} \quad (9)$$

Furthermore, \mathbf{R}_y can be represented as:

$$\mathbf{R}_y = \mathbf{\Phi}(\boldsymbol{\theta}) \text{diag}(\boldsymbol{\sigma}_s^2) \mathbf{\Phi}^H(\boldsymbol{\theta}) + \text{diag}(\boldsymbol{\sigma}_n^2) \quad (10)$$

Where $\boldsymbol{\sigma}_s^2 = [\sigma_{s1}^2, \sigma_{s2}^2, \dots, \sigma_{sK}^2]^H$ and $\boldsymbol{\sigma}_n^2 = [\sigma_n^2, \sigma_n^2, \dots, \sigma_n^2]^H$, $\mathbf{\Phi}(\boldsymbol{\theta})$ is the steering vector after

vector signal reconstruction of the single vector signal, which can be represented as:

$$\begin{aligned} \mathbf{\Phi}(\boldsymbol{\theta}) &= \mathbf{G}\mathbf{A}(\boldsymbol{\theta}) \\ &= \begin{bmatrix} 0 & 1 & -j \\ 1 & 0 & 0 \\ 0 & 1 & j \end{bmatrix} \begin{bmatrix} 1 & 1 & \dots & 1 \\ \cos(\theta_1) & \cos(\theta_2) & \dots & \cos(\theta_K) \\ \sin(\theta_1) & \sin(\theta_2) & \dots & \sin(\theta_K) \end{bmatrix} \\ &= \begin{bmatrix} e^{-j\theta_1} & e^{-j\theta_2} & \dots & e^{-j\theta_K} \\ 1 & 1 & \dots & 1 \\ e^{j\theta_1} & e^{j\theta_2} & \dots & e^{j\theta_K} \end{bmatrix} \\ &= [\mathbf{\Phi}(\theta_1), \mathbf{\Phi}(\theta_2), \dots, \mathbf{\Phi}(\theta_K)] \end{aligned} \quad (11)$$

In this processing, after the single vector received data undergoes vector signal reconstruction, its steering vector approximates that of a tri-element uniform linear array. This method not only preserves the key characteristics of the original signal but also provides a suitable mathematical structure for further signal processing and analysis. Assuming that DOA estimation is performed with T snapshots, then the received signal vector signal reconstruction model

$\mathbf{Y} = [\mathbf{y}(1), \mathbf{y}(2), \dots, \mathbf{y}(T)]$ can be represented as:

$$\mathbf{Y} = \Phi(\boldsymbol{\theta})\mathbf{S} + \mathbf{GN} \quad (12)$$

B. SPA Method

The SPA algorithm implements direction estimation using a reconstructed covariance matrix. This algorithm primarily solves the optimization problem of the covariance matrix through Semidefinite Programming (SDP) techniques. Notably, the SPA algorithm is suitable for covariance matrices with a Toeplitz structure, which is a key characteristic provided by the vector signal reconstruction method.

1. Covariance Fitting Criteria and SDP Formulations

The SPA method first estimates \mathbf{R}_y by re-parameterizing the above equation, and then determines the related parameters, defined as:

$$\mathbf{C}(\boldsymbol{\theta}, \boldsymbol{\sigma}_s^2) = \boldsymbol{\phi}(\boldsymbol{\theta}) \text{diag}(\boldsymbol{\sigma}_s^2) \boldsymbol{\phi}^H(\boldsymbol{\theta}). \quad (13)$$

The sparse and parametric estimation method first estimates \mathbf{R}_y by re-parameterizing the above equation, and then determines the related parameters, defined as:

$$\mathbf{C}_{il} = \sum_{k=1}^K \sigma_{sk}^2 \Phi_i(\theta_k) \Phi_l^*(\theta_k) = \sum_{k=1}^K \sigma_{sk}^2 e^{j\theta_k}. \quad (14)$$

Therefore, \mathbf{C} can be considered as a Hermitian-Toeplitz matrix composed of $M = 3$ complex numbers, expressed as $\mathbf{C} = T(\mathbf{u})$, where $\mathbf{u} \in \mathbb{C}^M$. The specific form is:

$$T(\mathbf{u}) = \begin{bmatrix} u_1 & u_2 & u_3 \\ u_2^* & u_1 & u_2 \\ u_3^* & u_2^* & u_1 \end{bmatrix} \quad (15)$$

Furthermore, the structure of the covariance matrix \mathbf{R}_y can be described as:

$$\mathbf{R}_y = T(\mathbf{u}) + \text{diag}(\boldsymbol{\sigma}_n^2) \quad (16)$$

In the context of a Uniform Linear Array (ULA), the covariance fitting criterion is based on the following prior assumption: For a ULA with M elements, it can detect up to $M - 1$ sources at most. For the single vector model after vector signal reconstruction, where $M = 3$, it is thus assumed that the maximum number of detectable sources $K \leq 2$.

The sample covariance matrix is defined as $\tilde{\mathbf{R}}_y = \frac{1}{N} \mathbf{Y} \mathbf{Y}^H$. Under the condition that both $\tilde{\mathbf{R}}_y$ and \mathbf{R}_y are invertible matrices, the covariance fitting criterion can be used for parameter estimation.

$$h_1 = \left\| \mathbf{R}_y^{-\frac{1}{2}} (\tilde{\mathbf{R}}_y - \mathbf{R}_y) \tilde{\mathbf{R}}_y^{-\frac{1}{2}} \right\|_{\text{F}}^2 \quad (17)$$

Therefore, the covariance fitting problem is transformed into a semidefinite programming (SDP) problem. Then, we obtain the following equivalent relation:

$$\min_{\mathbf{Q}, \mathbf{u}} \text{Tr}(\mathbf{Q}) + \text{Tr}(\tilde{\mathbf{R}}_y^{-1} T(\mathbf{u})), \text{subject to } \begin{bmatrix} \mathbf{Q} & \tilde{\mathbf{R}}_y^{\frac{1}{2}} \\ \tilde{\mathbf{R}}_y^{\frac{1}{2}} & T(\mathbf{u}) \end{bmatrix} \geq 0 \quad (18)$$

When $N < M$, $\tilde{\mathbf{R}}$ is a singular matrix, and an alternative covariance fitting criterion is used:

$$\begin{aligned} h_2 &= \text{tr} \left[(\tilde{\mathbf{R}}_y - \mathbf{R}_y) \mathbf{R}^{-1} (\tilde{\mathbf{R}}_y - \mathbf{R}_y) \right] \\ &= \text{tr}(\tilde{\mathbf{R}}_y \mathbf{R}_y^{-1} \tilde{\mathbf{R}}) + \text{tr}(\mathbf{R}_y) - 2 \text{tr}(\tilde{\mathbf{R}}_y) \end{aligned} \quad (19)$$

Based on this, a semidefinite programming (SDP) problem similar to the above can be constructed, with the specific form as follows:

$$\min_{\mathbf{Q}, \mathbf{u}} \text{tr}(\mathbf{Q}) + \text{tr}(T(\mathbf{u})), \text{subject to } \begin{bmatrix} \mathbf{Q} & \tilde{\mathbf{R}}_y \\ \tilde{\mathbf{R}}_y & T(\mathbf{u}) \end{bmatrix} \geq 0. \quad (20)$$

The constraint $T(\mathbf{u}) \geq 0$ is implicitly included in the constraints of the above equation. By solving one of the SDPs and given the solution \mathbf{u}^* , we can obtain $\hat{\mathbf{R}}_y = T(\mathbf{u}^*)$.

2. Direction of Arrival Solution

After obtaining $\hat{\mathbf{R}}_y$, the next step is to estimate the parameters $\boldsymbol{\theta}$. This study employs the Multiple Signal Classification (MUSIC) algorithm to address this issue:

$$\hat{\mathbf{R}}_y = \mathbf{U}_s \boldsymbol{\Sigma}_s \mathbf{U}_s^H + \mathbf{U}_N \boldsymbol{\Sigma}_N \mathbf{U}_N^H \quad (21)$$

\mathbf{U}_s represents the subspace formed by the eigenvectors corresponding to the larger eigenvalues, that is, the signal subspace. Conversely, \mathbf{U}_N is composed of the eigenvectors corresponding to the smaller eigenvalues, forming the noise subspace. Ideally, the signal subspace and the noise subspace in the data space are orthogonal to each other. Therefore, the spectral estimation formula of the MUSIC algorithm can be expressed as:

$$P(\theta) = \frac{1}{\mathbf{a}^H(\theta) \hat{\mathbf{U}}_N \hat{\mathbf{U}}_N^H \mathbf{a}(\theta)} \quad (22)$$

Here are the detailed implementation steps of the algorithm proposed in this article:

1. Single vector received data: \mathbf{X} .
2. Apply the vector signal reconstruction method to process the data, obtaining: \mathbf{Y} .
3. Based on the single vector signal after vector signal reconstruction, calculate the covariance matrix: $\hat{\mathbf{R}}_y$.
4. Optimize the reconstructed covariance matrix $\hat{\mathbf{R}}_y$ using semidefinite programming techniques.

5. Employ the MUSIC algorithm for the estimation of target angles.

IV. SIMULATION ANALYSIS

Considering a single vector hydrophone receiving K far-field targets, the SNR for the k th source under Gaussian noise is defined as:

$$\text{SNR} = 10 \log \left(\frac{E[|x_k(t)|^2]}{\sigma} \right), \quad k = 1, \dots, K. \quad (23)$$

The Root Mean Square Error (RMSE) of estimated DOAs is used to evaluate the accuracy of DOA estimation, RMSE is defined as:

$$\text{RMSE} = \sqrt{\frac{1}{KZ} \sum_{k=1}^K \sum_{z=1}^Z (\hat{\theta}_k^z - \theta_k^z)^2}, \quad (24)$$

Where θ_k^z represents the DOA of the k th source (true DOA) during the z th Monte Carlo simulation, $\hat{\theta}_k^z$ represents the estimated value for θ_k^z . Assuming the number of sources K is known, the positions of the K largest peaks are chosen as the estimated DOA values $\{\hat{\theta}_k^z\}_{k=1}^K$. The RMSE is the average over $Z = 400$ runs.

A. Single-Target Simulation

This section considers a single-target scenario, where the target's incidence angle is -30° , and the background noise is signal-independent complex Gaussian white noise. In the simulation, the number of snapshots is 1000, and the Signal-to-Noise Ratio (SNR) is set to 10dB and 0dB, respectively. The azimuth search step is 1° . This simulation compares the performance of Conventional Beamforming (CBF), Minimum Variance Distortionless Response (MVDR), MUSIC, Iterative Adaptive Approach (IAA)³⁰, SParse Iterative Covariance-based Estimation (SPICE)³¹, SPICE+³¹ algorithms, and VSRSPA, as shown in FIG. 1. The vertical red dashed line represents the

actual direction of incidence of the target, and all algorithms effectively estimated the target's direction. Notably, the CBF algorithm has the widest main lobe, while the VSRSPA algorithm shows the narrowest main lobe width and the lowest sidelobe level, displaying the sharpest peak. These characteristics are more pronounced at an SNR of 0dB.

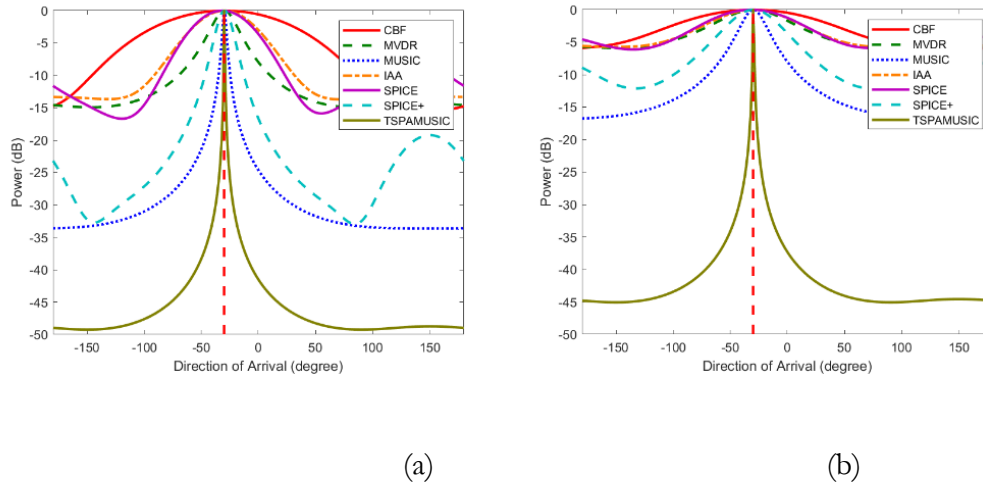


FIG. 1. Spatial Spectrum Graphs of Different DOA Algorithms for a Single Target:(a) SNR=10dB (b) SNR=0dB)

FIG. 2 shows the Root Mean Square Error (RMSE) curves of different DOA estimation algorithms under various SNR. In the context of a single target, the RMSE of azimuth estimation for all the aforementioned algorithms decreases as the SNR increases. When the SNR is less than -5dB, the RMSE rapidly increases with the improvement of signal SNR. For SNRs greater than -5dB, except for the SPICE algorithm, the RMSE of azimuth estimation for the other algorithms is less than 2° . When the SNR is above 0dB, except for the SPICE algorithm, the RMSE of azimuth estimation for the other methods is essentially consistent. When the SNR is below 0dB, the RMSE for the CBF, MVDR, IAA, SPICE+, and VSRSPA algorithms are basically the same, with the RMSE of the MUSIC algorithm being slightly higher than these algorithms.

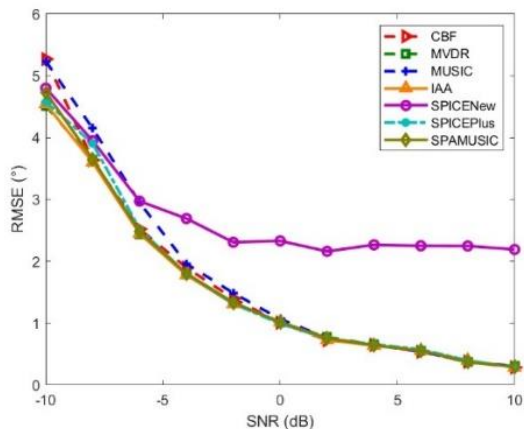
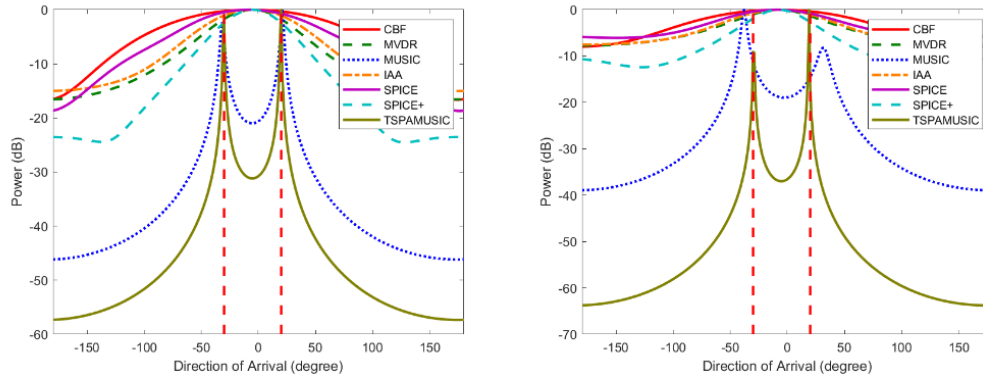


FIG. 2. Comparative Analysis of RMSE Performance for a Single-Target Scenario

B. Dual-Target Simulation

Considering a scenario with two targets, where the incident angles are $\theta_1 = -30^\circ$ and $\theta_2 = 20^\circ$, and the background noise is signal-independent complex Gaussian white noise. In the simulation, the number of snapshots is 1000, with SNRs of 10dB and 0dB. The azimuth search step is 1° . As shown in FIG. 3, in the context of dual targets, the azimuth spectra of CBF, MVDR, IAA, SPICE, and SPICE+ algorithms only display one peak, indicating that under these simulation conditions, these algorithms cannot distinguish between the two targets. However, at an SNR of 10dB, both the MUSIC algorithm and the Vector Signal Reconstruction Sparse and Parametric Approach (VSRSPA) can accurately estimate the positions of the targets, with the VSRSPA algorithm showing sharper peaks. When the SNR drops to 0dB, the estimation results of the MUSIC algorithm deviate significantly, with estimated angles of -45° and 35° , markedly different from the preset target positions. Meanwhile, the VSRSPA method still manages to accurately estimate the positions of the targets.



(a)

(b)

FIG. 3. Spatial Spectrum Estimation Comparison of Various Algorithms:(a) SNR=10dB (b) SNR=0dB

From the spatial spectrum above, it is evident that the CBF, MVDR, MUSIC, IAA, SPICE, and SPICE+ algorithms cannot distinguish between the two targets, hence the following images will not compare with the aforementioned algorithms. FIG. 4 shows the relationship between the RMSE of azimuth estimation and SNR for two targets using the MUSIC and VSRSPA algorithms. The MUSIC algorithm is represented by a blue dashed line, and below an SNR of -2dB, it cannot differentiate between the two targets, as the curve is not plotted for SNRs below -2dB. With increasing SNR, its RMSE significantly decreases, indicating improved estimation accuracy. Particularly, as the SNR increases from -10 dB to about 2 dB, the RMSE of the MUSIC algorithm rapidly decreases, then the decline rate slows but continues to decrease. The VSRSPA algorithm is represented by a green solid line, showing overall lower RMSE across all SNR levels compared to the MUSIC algorithm, indicating better performance within this test range. As the SNR increases, the RMSE of VSRSPA also shows a decreasing trend, and at high SNR values, its RMSE drops to near 0° , demonstrating higher positioning accuracy. It is evident from the graph that the

performance of both algorithms improves with increasing SNR, but the VSRSPA algorithm performs better than the MUSIC algorithm across the entire SNR range.

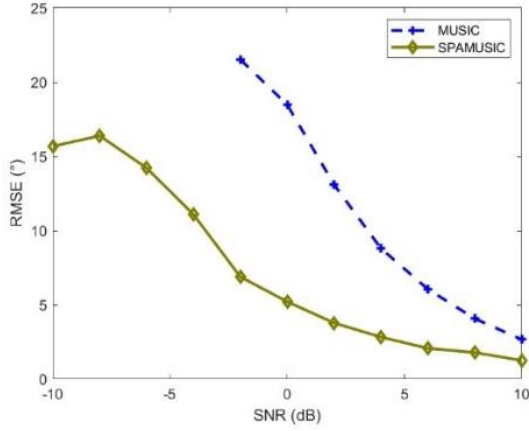


FIG. 4. Comparative Analysis of RMSE Performance for a Dual-Target Scenario

FIG. 5 shows the performance of the MUSIC algorithm and VSRSPA algorithm in terms of resolution probability at different SNR levels. The horizontal axis represents the SNR in decibels (dB), ranging from -10 dB to 10 dB. The vertical axis represents the resolution probability, from 0 to 1. In the graph, the MUSIC algorithm is represented by a blue dashed line, with its performance improving as the SNR increases, but with slower performance growth under low SNR conditions. The VSRSPA algorithm is represented by a green solid line, displaying higher resolution probability across the entire SNR range, especially when the SNR is greater than -4dB, approaching 1, indicating superior performance compared to the MUSIC algorithm.

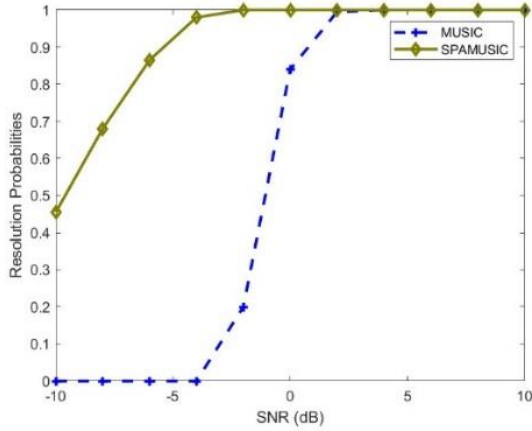


FIG. 5. Comparative Analysis of Resolution Probability for a Dual-Target Scenario

V. CONCLUSION

In this paper, we explored the application of single vector hydrophones in underwater acoustic signal processing for DOA estimation. Addressing the challenges faced by traditional DOA estimation methods, such as multi-source signals and noise interference, we proposed the VSRSPA algorithm. Through theoretical analysis and simulation experiments, we demonstrated that the VSRSPA algorithm can effectively improve the accuracy and resolution of DOA estimation, especially outperforming traditional methods in low SNR and multi-source environments. This study also facilitated the application and further research of sparse signal processing algorithms, such as atomic norm minimization, on single vector hydrophones by reconstructing the single vector signal model.

REFERENCES

- ¹A. Bereketli, M. B. Guldogan, T. Kolcak, T. Gudu, and A. L. Avsar, “Experimental Results for Direction of Arrival Estimation with a Single Acoustic Vector Sensor in Shallow Water,” *J. Sens.* **2015**, 1–10 (2015).
- ²J. P. Ryan, K. J. Benoit-Bird, W. K. Oestreich, P. Leary, K. B. Smith, C. M. Waluk, D. E. Cade, J. A. Fahlbusch, B. L. Southall, J. E. Joseph, T. Margolina, J. Calambokidis, A. DeVogelaere, and J. A. Goldbogen, “Oceanic giants dance to atmospheric rhythms: Ephemeral wind-driven resource tracking by blue whales,” *Ecol Lett* **25**, 2435–2447 (2022).
- ³K. B. Smith, P. Leary, T. Deal, J. Joseph, J. Ryan, C. Miller, C. Dawe, and B. Cray, “Acoustic vector sensor analysis of the Monterey Bay region soundscape and the impact of COVID-19,” *J. Acoust. Soc. Am.* **151**, 2507 (2022).
- ⁴X. Zhang, G. Zhang, Z. Shang, S. Zhu, P. Chen, R. Wang, and W. Zhang, “Research on DOA Estimation Based on Acoustic Energy Flux Detection Using a Single MEMS Vector Hydrophone,” *Micromachines* **12**, 168 (2021).
- ⁵P. Vallet, X. Mestre, and P. Loubaton, “Performance Analysis of an Improved MUSIC DoA Estimator,” *IEEE Trans. Signal Process.* **63**, 6407–6422 (2015).
- ⁶Y. Ning, S. Ma, F. Meng, and Q. Wu, “DOA Estimation Based on ESPRIT Algorithm Method for Frequency Scanning LWA,” *IEEE Commun. Lett.* **24**, 1441–1445 (2020).
- ⁷G. L. D’Spain, W. S. Hodgkiss, G. L. Edmonds, J. C. Nickles, F. H. Fisher, and R. A. Harriss, “Initial Analysis Of The Data From The Vertical DIFAR Array,” in *OCEANS 92 Proceedings@M_Mastering the Oceans Through Technology*, Vol. 1 (1992), pp. 346–351.

- ⁸X. Wang, J. Chen, J. Han, and Y. Jiao, "Optimization for the direction of arrival estimation based on single acoustic pressure gradient vector sensor," *Int. J. Nav. Archit. Ocean Eng.* **6**, 74–86 (2014).
- ⁹P. Tichavsky, K. T. Wong, and M. D. Zoltowski, "Near-field/far-field azimuth and elevation angle estimation using a single vector hydrophone," *IEEE Trans. Signal Process.* **49**, 2498–2510 (2001).
- ¹⁰D. Levin, E. A. P. Habets, and S. Gannot, "Maximum likelihood estimation of direction of arrival using an acoustic vector-sensor," *J. Acoust. Soc. Am.* **131**, 1240–1248 (2012).
- ¹¹G. Liang, K. Zhang, J. Fu, Y. Zhang, and L. LI, "Research on high-resolution direction-of-arrival estimation based on an acoustic vector-hydrophone," *Acta Armamentarii.* **32**, 986 (2011).
- ¹²A. Liu, D. Yang, S. Shi, and Z. Zhu, "MUSIC-based direction of arrival estimation methods with virtual source elimination for single vector sensor in isotropic ambient noise," *Chin. J. Acoust.* **38**, 459–473 (2019).
- ¹³Y. Chen, W. Wang, J. Wang, S. Ma, and Z. Meng, "Research on high-resolution direction-of-arrival estimation of a single vector hydrophone with noise," *J. Harbin Eng. University* **34**, 65–70 (2013).
- ¹⁴Y. Park, Y. Choo, and W. Seong, "Multiple snapshot grid free compressive beamforming," *J. Acoust. Soc. Am.* **143**, 3849 (2018).
- ¹⁵X. Wu, W. Zhu, and J. Yan, "A Toeplitz Covariance Matrix Reconstruction Approach for Direction-of-Arrival Estimation," *IEEE Trans. Veh. Technol.* **66**, 8223–8237 (2017).
- ¹⁶Z. Yang, L. Xie, and C. Zhang, "A Discretization-Free Sparse and Parametric Approach for Linear Array Signal Processing," *IEEE Trans. Signal Process.* **62**, 4959–4973 (2014).

- ¹⁷G. Zhang, K. Liu, J. Fu, and S. Sun, “Covariance matrix reconstruction method based on amplitude and phase constraints with application to extend array aperture,” *J. Acoust. Soc. Am.* **151**, 3164 (2022).
- ¹⁸C. Zhou, Y. Gu, X. Fan, Z. Shi, G. Mao, and Y. D. Zhang, “Direction-of-Arrival Estimation for Coprime Array via Virtual Array Interpolation,” *IEEE Trans. Signal Process.* **66**, 5956–5971 (2018).
- ¹⁹B. N. Bhaskar, G. Tang, and B. Recht, “Atomic Norm Denoising With Applications to Line Spectral Estimation,” *IEEE Trans. Signal Process.* **61**, 5987–5999 (2013).
- ²⁰H. Abeida, Q. Zhang, J. Li, and N. Merabtine, “Iterative Sparse Asymptotic Minimum Variance Based Approaches for Array Processing,” *IEEE Trans. Signal Process.* **61**, 933–944 (2013).
- ²¹C. Li, G. Liang, L. Qiu, T. Shen, and L. Zhao, “An efficient sparse method for direction-of-arrival estimation in the presence of strong interference,” *J. Acoust. Soc. Am.* **153**, 1257 (2023).
- ²²C. Wang, L. Da, M. Han, Q. Sun, and W. Wang, “Sparse asymptotic minimum variance based bearing estimation algorithm for a single vector hydrophone,” *Chin. J. Acoust.* **41**, 35–48 (2022).
- ²³P. Chen, Z. Chen, Z. Cao, and X. Wang, “A New Atomic Norm for DOA Estimation With Gain-Phase Errors,” *IEEE Trans. Signal Process.* **68**, 4293–4306 (2020).
- ²⁴M. Fu, Z. Zheng, K. Zhang, and W.-Q. Wang, “Coarray Interpolation for Direction Finding and Polarization Estimation Using Coprime EMVS Array via Atomic Norm Minimization,” *IEEE Trans. Veh. Technol.* **72**, 10162–10172 (2023).
- ²⁵Y. Li and Y. Chi, “Off-the-Grid Line Spectrum Denoising and Estimation With Multiple Measurement Vectors,” *IEEE Trans. Signal Process.* **64**, 1257–1269 (2016).

- ²⁶Z. Yang and L. Xie, “On Gridless Sparse Methods for Line Spectral Estimation From Complete and Incomplete Data,” *IEEE Trans. Signal Process.* **63**, 3139–3153 (2015).
- ²⁷Z. Yang and L. Xie, “Enhancing Sparsity and Resolution via Reweighted Atomic Norm Minimization,” *IEEE Trans. Signal Process.* **64**, 995–1006 (2016).
- ²⁸J. Hui, H. Liu, H. Yu, and M. Fan, “Study on the physical basis of pressure and particle velocity combined processing,” *Chin. J. Acoust.* **25**, 303–307 (2000).
- ²⁹Z. Yao, K. Jiang, R. Guo, and Y. Chen, “An improved bearing estimation algorithm using acoustic vector sensor array based on rotational invariance technique,” *Transactions of Beijing institute of Technology*, 513-516,521 (2012).
- ³⁰T. Yardibi, J. Li, P. Stoica, M. Xue, and A. B. Baggeroer, “Source Localization and Sensing: A Nonparametric Iterative Adaptive Approach Based on Weighted Least Squares,” *IEEE Trans. Aerosp. Electron. Syst.* **46**, 425–443 (2010).
- ³¹P. Stoica, P. Babu, and J. Li, “SPICE: A Sparse Covariance-Based Estimation Method for Array Processing,” *IEEE Trans. Signal Process.* **59**, 629–638 (2011).